Available online at www.sciencedirect.com

SCIENCE DIRECT®

Vision Research 44 (2004) 3347–3355

Vision Research

www.elsevier.com/locate/visres

L-type calcium channel agonist induces correlated depolarizations in mice lacking the β2 subunit nAChRs

Christine Torborg, Chih-Tien Wang, Gianna Muir-Robinson, Marla B. Feller *

Neurobiology Section 0357, Division of Biological Sciences, UCSD, 9500 Gilman Drive, La Jolla, CA 92093-0357, USA

Received 4 June 2004; received in revised form 23 July 2004

Abstract

Retinal waves are mediated in part by activation of nicotinic receptors containing the β2 subunit. Mice deficient in β2 containing nAChRs have maintained firing of action potentials but do not support correlated waves. As a result, β2−/− mice have inhibited refinement of circuits within the retina as well as retinal projections to the CNS. Previously, we observed that correlated increases in calcium reminiscent of retinal waves could be induced in β2−/− retina by pharmacological application of the L-type calcium channel agonist, FPL-64176. Here, we characterize FPL-induced activity patterns in β2−/− retina using both whole cell and multielectrode array recordings. FPL-induced strong depolarizations in previously non-spiking β2−/− retinal ganglion cells. Though these strong depolarizations were likely to underlie the FPL-induced calcium transients, they led to highly variable effects on the spiking of individual retinal ganglion cells. In addition, induced spiking activity had significantly weaker nearest-neighbor correlations than WT mice. Initial attempts of intraocular injections of FPL in β2−/− mice did not rescue eye-specific layer formation. These findings indicate that activity induced by FPL is not sufficient for driving eye-specific segregation in β2−/− mice.

Abbreviations: $[Ca^{2+}]_i$ intracellular calcium concentration; dLGN dorsal lateral geniculate nucleus; nAChR nicotinic acetylcholine receptor; RGC retinal ganglion cell; WT wild-type

1. Introduction

Spontaneous activity in the developing retina occurs as waves of action potentials with specific spatiotemporal properties. These waves occur before eye opening, and are required for segregation of retinal ganglion cell (RGC) axons into eye-specific layers in the dLGN (Penn, Riquelme, Feller, & Shatz, 1998; Sretavan, Shatz, & Stryker, 1988) and retinotopic refinement of retinocollicular axons (McLaughlin, Torborg, Feller, & O'Leary, 2003). The question remains—what are the salient features of the firing patterns induced by waves for driving this process?

To address this question, both pharmacological (Huberman et al., 2003; Stellwagen & Shatz, 2002) and genetic manipulations have been developed that significantly alter the endogenous pattern of retinal activity without completely blocking it. One transgenic mouse that has been utilized by several labs is the mouse lacking the β2 subunit of the nAChR (Picciotto et al., 1995; Xu et al., 1999). β2−/− mice do not exhibit retinal waves during the first postnatal week, but have normal spontaneous retinal activity in the second (Bansal, Singer, Hwang, & Feller, 2000). Although waves are absent in β2−/− mice during the first postnatal week, RGCs continue to fire uncorrelated action potentials (McLaughlin et al., 2003). Hence, β2−/− mice are an excellent model system for studying the role of correlated firing patterns in driving activity-dependent processes in visual system development.

* Corresponding author. Tel.: +1 858 8224273; fax: +1 858 5347309.
E-mail address: mfeller@ucsd.edu (M.B. Feller).

0042-6989/$ - see front matter © 2004 Elsevier Ltd. All rights reserved.
doi:10.1016/j.visres.2004.08.015

Several alterations have been characterized in the developing visual system of β2−/− mice. First, though their retinas are grossly normal, segregation of RGC dendrites into ON and OFF sublamina is delayed (Bansal et al., 2000). Second, retinotopic refinement of β2−/− RGC projections to the superior colliculus is inhibited into adulthood (McLaughlin et al., 2003), indicating that in contrast to RGC dendritic development, the first postnatal week represents a critical period during which retinal waves drive the establishment of topographic maps. Third, β2−/− RGC projections to the lateral geniculate nucleus (dLGN) never form eye-specific layers (Muir-Robinson, Hwang, & Feller, 2002; Rossi et al., 2001), though RGC axons segregate locally after retinal waves are restored during the second postnatal week (Muir-Robinson et al., 2002). In vivo recordings from dLGN neurons in adult β2−/− mice reveal that even in the absence of eye-specific layers, individual dLGN neurons are driven by only one eye (Grubb, Rossi, Changeux, & Thompson, 2003), indicating eye-specific segregation is comparable to WT mice. Fourth, in vivo recordings also revealed that there was an inhibition in the fine topography of β2−/− retinogeniculate projections along the nasal–temporal axis (Grubb et al., 2003). Fifth, in β2−/− mice, retinogeniculate axons are organized into ON- or OFF-center domains, implying that altered activity patterns may lead to the establishment of a functional map not observed in WT mice (Grubb et al., 2003). Sixth, visually-evoked field potentials in primary visual cortex of β2−/− mice show an increased size of the binocular zone and decrease in acuity (Rossi et al., 2001).

The interpretations of experiments conducted with β2−/− mice have been based mostly on the assumption that the effects are due to changes in RGC firing properties. However, the observed changes in the visual system circuitry may be a result of developmental compensation that has been induced by the absence of β2-containing nAChRs either in the retina or its target structures. Several recent results are consistent with the interpretation that these multiple phenotypes in β2−/− mice are due to changes in retinal firing pattern. Intraocular injections of nAChR antagonists prevent the formation of eye-specific layers (Huberman, Stellwagen, & Chapman, 2002; Huberman et al., 2003; Penn et al., 1998; Rossi et al., 2001), implying that disruption in retinal activity is sufficient to explain the disruption of eye-specific segregation observed in β2−/− mice. In addition, application of a general nAChR antagonist directly to the dLGN (Penn et al., 1998) or the superior colliculus (Simon, Prusky, O'Leary, & Constantine-Paton, 1992) does not alter map refinement in either target, also consistent with the interpretation that the inhibition of map refinement observed in β2−/− mice was due to changes in retinal waves.

A powerful approach to address whether changes in visual system circuitry are due to altered retinal spiking patterns would be to rescue the effects on visual system development by inducing waves in β2−/− mice. Previously, it was demonstrated that exposing retinas to the L-type calcium channel agonist FPL induces propagating waves in the absence of fast synaptic transmission (Singer, Mirotznik, & Feller, 2001). Indeed, FPL induces waves in β2−/− mice as assayed by fluorescence imaging of calcium indicators (Singer et al., 2001). However, the ability to rescue map defects in β2−/− mice may depend on the ability of FPL to induce the appropriate pattern of spiking activity in vivo.

Here we characterize the effects of FPL on the spiking properties of RGCs using whole cell recording and a multielectrode array. We also conduct intraocular injections of FPL in β2−/− mice to assay whether the presence of FPL rescues eye-specific segregation of retinogeniculate axons.

2. Methods

2.1. Retinal preparation

All procedures were performed in accordance with approved animal use protocols. Retinas were isolated as described previously (Bansal et al., 2000). Briefly, newborn mice (P1–P5) were anesthetized with halothane and decapitated. Retinas were isolated in cold (4 °C) artificial cerebrospinal fluid (ACSF) containing (in mM): 119.0 NaCl, 26.2 $NaHCO_3$, 11 glucose, 2.5 KCl, 1.0 K_2HPO_4, 2.5 $CaCl_2$ and 1.3 $MgCl_2$. Retinas were cut into thirds and mounted, ganglion cell side up, onto filter paper. These whole mount preparations were kept at 32 °C in ACSF bubbled with 95% O_2/5% CO_2 until use (1–6 h). During experiments, all preparations were superfused continuously with oxygenated ACSF warmed to 32 °C.

2.2. Electrophysiology

Whole cell current-clamp recordings were made from visualized ganglion cells (40× water-immersion objective; Olympus Optical). Borosilicate glass pipettes (Garner Glass Co., Claremont, CA) were pulled (PP-830, Narishige) to a tip resistance of ~5 MΩ when filled with an internal solution containing (in mM): 98.3 potassium gluconate, 40 HEPES, 1.7 KCl, 0.6 EGTA, 5 $MgCl_2$, 2 Na_2ATP, and 0.3 Na-GTP; pH was adjusted to 7.25 with KOH. For whole-cell voltage clamp, the current responses to FPL-64176 (Sigma F131) were recorded at a membrane potential of −60 mV. Data were filtered at 1 kHz and digitized at 5 kHz. For whole-cell current clamp, the membrane potential changes were monitored with no current injected. In successful recordings, seals >1 *G*Ω were obtained in 30 s or less. The ratios of the access resistance to the input resistance were 5–15% before

and after FPL application. Recordings were made using an Axopatch 200B patch-clamp amplifier (Axon Instruments; Foster City, CA), and data were acquired to and analyzed on a Pentium based PC using PClamp 6.0 software (Axon Instruments).

2.3. Multielectrode recordings and analysis

A retinal piece from either P4 WT or β2−/− mice was placed ganglion cell side down onto a flat, hexagonal array of 61 extracellular electrodes spaced 60 μm apart from each other, with a total diameter of 480 μm. The retina was held down on the array by placing a platinum ring on the filter paper. During recording the retina was continuously perfused with oxygenated ACSF and the bath temperature was 36 °C. 2.88 mM FPL in ethanol was added to the ACSF in a 1:1000 dilution for a final concentration of 2.88 μM.

Spike times, peaks, and widths were digitized with a temporal resolution of 0.05 ms (Meister, Pine, & Baylor, 1994) and then stored for off-line analysis. Spikes were manually segregated into single units by selecting distinct clusters in scatter plots of spike height and width recorded on each electrode (Meister et al., 1994) and verifying the presence of a refractory period in the spike trains from each cluster. Spikes recorded on multiple electrodes were identified by temporal coincidence; only spikes from the electrode with the most clearly defined cluster were further analyzed. Using this method, between 5 and 10 unique units were identified from each retina piece. Cells were considered to be at the position of the electrode on which they were recorded.

We computed several measures of the spiking properties of RGCs for each single unit recorded. The median firing rate was calculated by first calculating the instantaneous firing rate for all spikes recorded for an individual unit, then determining the median for that unit. The average number of action potentials was calculated by summing the total number of action potentials for each 20 min recording and then dividing by the length of the recording. The percentage of time cells were firing was calculated by summing the interspike intervals (ISI) less than either 1 s or 100 ms and dividing this by the total time of the recording. Correlation index was calculated as previously described (Wong, Meister, & Shatz, 1993; McLaughlin et al., 2003). Briefly, this was calculated by determining the number of spikes from cell A that occurred within ±100 ms of a spike in cell B and then dividing this by the number of spike pairs that would have occurred by random chance. Since firing rates were often very different between both cells in a pair, the correlation index was calculated using both NAB and NBA. Since the distributions for each parameter measure were non-normal, averages were reported as medians. For statistical analysis, units from each condition (WT retinas, β2−/− retinas in the presence of FPL) were grouped. A chi-square median test (JMP5.1) was used to compare β2−/− retinas in the presence of FPL to WT. *P*-values less than 0.05 were taken as significant. All other analysis was performed using IgorPro (Wavemetrics, Inc).

2.4. Visualization of retinogeniculate projections

All surgeries on mouse pups were performed according to institutional guidelines and approved protocols. Mice were anaesthetized with 3.5% isoflurane/2%O_2. The eyelid was cut open to expose the temporal portion of the eye, and 0.1–1 μl of 5% β-choleratoxin conjugated to either FITC or TRITC was injected into the retina with a fine glass micropipette with a picospritzer (WPI). β-Choleratoxin is transported throughout RGCs, clearly labeling axons and terminals. Twenty-four hours later, mice were heavily anaesthetized with an overdose of isoflurane. After fixation by cardiac perfusion with 4% paraformaldehyde in PBS, brains were sectioned to 100 μ on a Vibratome.

Images were analyzed as described previously (Muir-Robinson et al., 2002; Torborg & Feller, 2004). Briefly, eight-bit tagged image file format images were acquired for FITC- or TRITC-labeled sections of the LGN with a CCD camera (Optronics, Goleta, CA) attached to an upright microscope (Zeiss Axioscope 2; Thornwood, NY) with a 10× objective (numerical aperture, 0.45). The three sections that contained the largest ipsilateral projection, corresponding to the central third of the LGN were selected, and all analysis was performed on these sections on the side of the brain with an FITC-labeled ipsilateral/TRITC-labeled contralateral projection.

For each pixel, we computed the logarithm of the intensity ratio, $R = \log_{10}(F_I/F_C)$, where F_I is the ipsilateral channel fluorescence intensity and F_C is the contralateral channel fluorescence intensity. We then calculated the variance of the distribution of *R*-values for each section, which was used to compare the width of the distributions across mice. Wider distributions of *R* indicate more contra- and ipsi-dominant pixels, and therefore more segregation.

2.5. Intraocular injections of FPL

FPL-64176 stock was prepared as concentrated stock solution of 2.88 mM in 100% ethanol and diluted in sterile saline before intraocular injections. We injected binocularly with 0.5–1 μl of solution containing 20–100 μM FPL. Injections were made in the temporal portion of the eye at the level of the ora serrata. Injections were made every 48 h, at P2, P4 and P6 with a dye injection at P7. Brains were processed as described above. To determine whether repeated injections caused damage to the retina, we looked at several parameters (Supplemental Figure 1). First, we recorded from RGCs in a retina that had received an injection of control substances

18 h previously. We found that this retina had normal resting membrane potentials and exhibited normal waving activity ($n = 5$ cells, 3 retinas). Second, we examined retinas that had undergone the full set of injections and found there was no apparent structural damage to RGCs. This control was conducted for mice receiving eye injections of either control substances or FPL ($n = 10$). After 8 days of FPL treatment, washout of the drug restored retinal waves in acutely isolated WT retina as assessed by calcium imaging ($n = 3$). Third, the retina projection to the colliculus contralateral to the eye that had received multiple injections was complete, indicating that the entire retina was equally able to transport dye to its targets. This control was conducted for mice receiving eye injections of either control substances or FPL ($n = 10$). Fourth, we found that WT mice receiving eye injections of control substances had normal eye-specific segregation, also indicating that neither the ipsilateral or contralateral projecting RGCs were damaged ($n = 6$).

3. Results

3.1. L-type calcium channel agonist can induce activity in β2−/− mice

Mice lacking the β2 subunit of nAChRs lack retinal waves between P1 and P8 (Bansal et al., 2000). In WT mice, bath application of FPL-64176, an L-type calcium channel agonist, induces large, frequent, rapidly propagating waves and these waves persisted in the presence of antagonists of nicotinic acetylcholine, ionotropic glutamate, $GABA_A$, and glycine receptors that have been shown to mediate or modulate retinal waves in a variety of preparations (Singer et al., 2001). Using fluorescent imaging of fura-2 in β2−/− mice, we found that bath application of FPL induced frequent, propagating waves (Fig. 1, $n = 4$) as described previously (Singer et al., 2001).

Whole-cell current clamp recordings from individual RGCs showed that bath application of FPL induced periodic spontaneous depolarizations in β2−/− RGCs (Fig. 2). The levels of these spontaneous depolarizations ranged from 7 to 30 mV with a mean of 18.7 ± 4.0 mV (±SE; 6 cells from 6 retinas) and occasionally reached a plateau (e.g. the first depolarization in the left trace of Fig. 2A). Since FPL had no significant effects on resting membrane potential (−51 ± 1.4 mV for control and −54 ± 3.2 mV for FPL, 6 RGCs from 6 retinas), these FPL-induced depolarizations were not due to an overall increase in excitability of the neurons.

Whole-cell voltage clamp recordings from the same groups of cells showed that periodic spontaneous synaptic currents were also induced by bath application of FPL (Fig. 2B), implying that these currents were driving the depolarizations. The inter-event interval of these

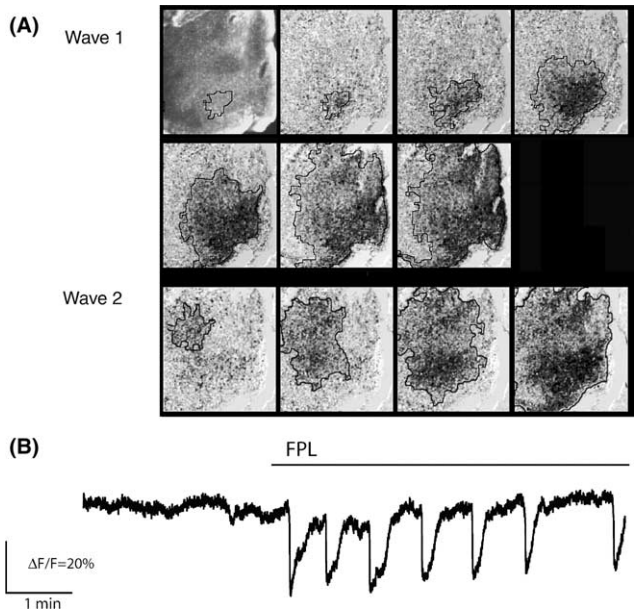

Fig. 1. Retinal waves are induced in β2−/− mice by bath application of the L-type calcium channel agonist, FPL. (A) Time evolution of two retinal waves induced in β2−/− retina by bath application of the L-type calcium channel agonist FPL (2 μM). First frame in upper left is fluorescence image of β2−/− retina incubated in the calcium indicator, fura-2AM. Each frame represents successive 0.5 s intervals. Second wave occurs 10 s after first wave. (B) The time course of fractional change in fura-2 fluorescence ($\Delta F/F$) associated with waves averaged over a 200 μm^2 area before and during bath application of 2.5 μM FPL. Downward deflections in fluorescence correspond to increases in intracellular calcium concentration.

spontaneous currents was not distinguishable from that of the spontaneous depolarizations (Fig. 2C), suggesting that a single depolarization may correspond to the occurrence of a single compound synaptic current. The identity of this depolarizing current is not yet known.

After FPL application, β2−/− RGCs lost their ability to fire in response to the injected current steps (Fig. 2D and E). The computed slopes from the linear fits to the input–output relationship decreased from 0.83 ± 0.03 to 0.15 ± 0.02 action potentials/pA in the presence of FPL. The reduction in the slope of the RGC input–output curves in the presence of FPL is unexplained. From the experiments described in the section below, it is clear retinal neurons can continue to fire action potentials in the presence of FPL therefore we do not think that FPL acts non-specifically on voltage-gated Na^+ channels. One possibility is that the strong calcium influx induced by FPL may have led to a rapid washout of Na^+ channels during whole cell recordings.

3.2. L-type calcium channel agonists induce spiking patterns in β2−/− mice that differ significantly from WT spiking patterns

In contrast to the whole cell experiments described above, an extracellular multielectrode array selects only

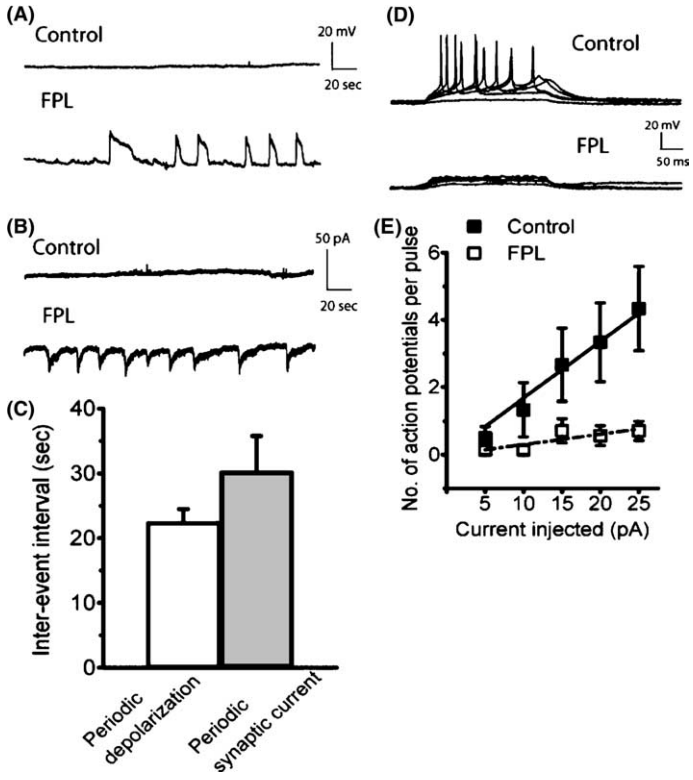

Fig. 2. FPL induced periodic spontaneous depolarizations and synaptic currents in β2−/− mice (A). Spontaneous depolarizations are measured during continuous whole-cell current clamp recordings from a presumptive retinal ganglion cell in the absence and presence of 2.5 μM FPL. (B) Synaptic currents are measured during continuous whole-cell voltage clamp recordings from the same cells as part A. Cell is held at −60 mV. (C) Summary data of inter-event intervals measured from spontaneous depolarizations and spontaneous synaptic currents recorded in the presence of FPL. (D) Membrane voltage responses to current steps were recorded in the absence (top) and presence (bottom) of FPL. Five step-pulsed currents in series were injected into RGCs with 250 ms duration for each pulse. The intervals between steps were 3 s. The steps ranged from 5 to 25 pA with steps on 5 pA. (E) Summary input–output curves plotting the number of action potentials per pulse vs. current injected using the pulse protocol in D.

those neurons that spike. Using a multielectrode array, we assayed the effects of FPL on the spiking patterns of many β2−/− retinal neurons simultaneously. P4 WT retinal neurons fire bursts of action potentials that are correlated among neighboring cells and are separated by long periods of silence (McLaughlin et al., 2003; Fig. 3A, top). Previously, we showed that β2−/− retinal neurons fire bursts of action potentials that have an instantaneous firing rate of approximately 5 Hz and these bursts are uncorrelated across neighboring neurons (Torborg, Hansen, & Feller, 2004). In contrast, in the presence of FPL, many β2−/− retinal neurons fired bursts of correlated action potentials; however, some cells fired tonically and others fired only single spikes (Fig. 3A, bottom).

To determine whether FPL induced activity patterns that could potentially rescue eye-specific segregation, we compared several parameters of the spiking patterns between WT ($n = 2$ retinas, 16 cells) and FPL-induced activity in β2 neurons (β2−/− FPL) ($n = 2$ retinas, 17 cells). On average, the total number of spikes was increased in β2−/− FPL retinas relative to WT retinas ($p < 0.01$) (Fig. 3B); however, these spikes occurred at similar instantaneous firing rates in β2−/− FPL retinas and WT retinas ($p = 0.39$) (Fig. 3C). Even though the average instantaneous firing rate was similar in β2−/− FPL retinas, the increased number of spikes meant that the percentage of time that cells were firing at greater than 1 Hz was increased relative to WT ($p < 0.01$) (Fig. 3D) but that the percentage of time spent firing at greater than 10 Hz (Fig. 3E) was not significantly different between β2−/− FPL retinas and WT retinas ($p = 0.058$). Notably, all measures were more variable in β2−/− FPL than WT.

We also assayed the strength of correlation between cells by computing the correlation index (a measure of the number of spikes correlated within ±100 ms between a pair of cells relative to that expected by chance). Although β2−/− FPL neurons appeared to fire in correlated bursts, the correlation index was significantly reduced relative to WT. In WT retinas, the correlation index decreased as a function of distance between cell pairs ($p < 0.001$) (Fig. 3F, left). However in β2−/− FPL retinas, the correlation index did not change as a function of distance ($p = 0.096$) (Fig. 3F, right), and is decreased relative to WT in cell pairs that were less than

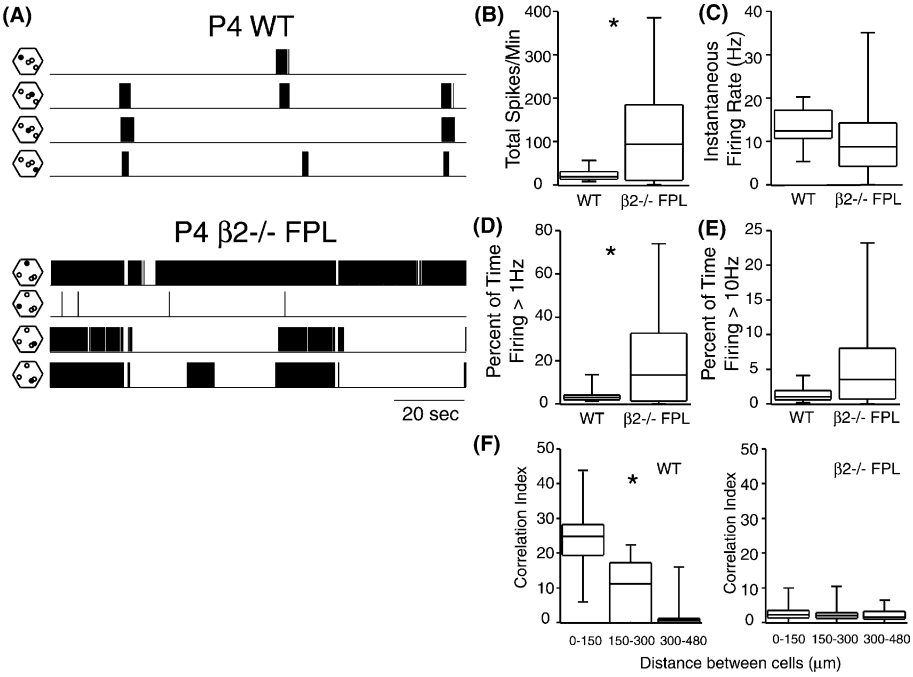

Fig. 3. FPL induced spiking in β2−/− retinas that differed from WT spiking patterns. Spontaneous action potentials were recorded on a hexagonal array of 61 electrodes spaced 60 μm apart. Individual units were identified by manually selecting clusters of spikes with similar heights and widths. Asterisks indicate medians are significantly different ($p < 0.05$). (A) Representative spike trains recorded from four different sorted units from a P4 WT retina and a P4 β2−/− retina in the presence of 2.88 μM FPL. Hexagons to the left of each spike train show the position of the electrode on which that unit was recorded (filled circles) relative to the other units (open circles). For (B)–(F) the box plots represent the following measures. The center line is the median data point; the box represents the center 50% of data points, and the bars represent the entire range of the distribution of data points. (B) Box plots of the total number of spikes/min. (C) Box plots of the instantaneous firing rate. (D) Box plots of the percentage of time that individual retinal neurons were firing at greater than 1 Hz. (E) Box plots of the percentage of time that individual retinal neurons were firing at greater than 10 Hz. (F) Box plots of the correlation index. Since in WT retinas, cells that nearby are more correlated than more distant cell pairs, cells were grouped according to the distance between the electrodes on which those cells were recorded (0–150 μm, 151–300 μm, and 301–500 μm).

300 μm apart ($p < 0.05$). For more distant cell pairs, there was almost no correlation in WT cells; however, there was a small amount of correlation in β2−/− FPL retinas. These data indicate that the pattern of spikes in β2−/− cells in the presence of FPL was dramatically different in both temporal and spatial structure from the spiking patterns in WT cells.

3.3. Intraocular injection of FPL does not rescue eye-specific segregation

The above results indicate that although L-type calcium channel agonists induced correlated increases in intracellular calcium concentration ($[Ca^{2+}]_i$) in β2−/− mice, the resulting spiking patterns were significantly more variable and less spatially correlated than the patterns in WT mice. As a first attempt to determine whether FPL-induced depolarizations could rescue eye-specific layer segregation in β2−/− mice, we performed repeated binocular injections of FPL in β2−/− mice ($n = 4$ mice). Injection concentrations varied between 20 and 100 μM and repeated 1–2 times in the first postnatal week. The number and size of the injections were limited by the toxicity of FPL. Retinogeniculate projection patterns were assayed by intraocular injection of the fluorescent tracer β-choleratoxin. The extent of segregation is assayed by the width of *R*-values distribution for each set of images where *R* is defined as the logarithm of the intensity ratio, $R = \log_{10}(F_I/F_C)$, where F_I is the ipsilateral channel fluorescence intensity and F_C is the contralateral channel fluorescence intensity (Fig. 4B, see Section 2).

As reported previously β2−/− dLGN are much less segregated at P8 than WT (Muir-Robinson et al., 2002; Torborg & Feller, 2004). Projection patterns differ significantly between P8 WT and β2−/− mice in that β2−/− ipsilateral fibers do not coalesce to form a coherent layer and there is no decrease of intensity in the contralateral projection at the location of ipsilateral fibers (Fig. 4A). We found that the presence of FPL in β2−/− mice did not enhance eye-specific segregation but rather inhibited it significantly (Fig. 4B). Assuming that the effects of FPL on the retina were similar in vivo as in vitro (Figs. 1 and 2), this finding is consistent with the hypothesis that FPL-induced $[Ca^{2+}]_i$ transients or spiking are not sufficient to drive eye-specific segregation.

As a control for assaying the in vivo effects of intraocular injections of FPL, we conducted binocular injections

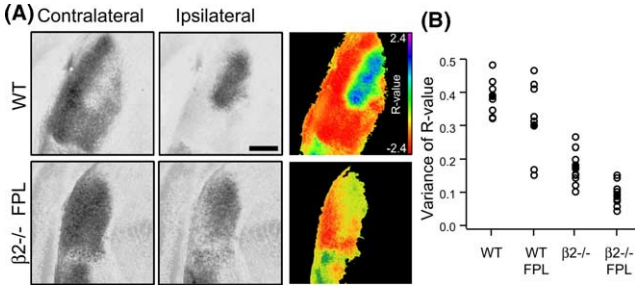

Fig. 4. Intraocular FPL injections does not rescue eye-specific layer formation and segregation in the dLGN of β2−/− mice. (A) Fluorescence images of contralateral (column 1) and ipsilateral (column 2) projections in the same dLGN coronal section (100 μm thick). (column 3) Images of the dLGN pseudocolored according to the *R*-value for each pixel where $R = \log_{10}(F_I/F_C)$. Scale bar = 200 μm. (B) Summary of the variance of the *R* distributions for each image. Open circles are the variance of the *R* distribution for each section, and closed circles are the mean variances for all sections.

of FPL into WT mice. Since WT mice were not as sensitive to the toxic effects of FPL as β2−/− mice, injection concentrations varied between 50–100 μM and repeated three times in the first postnatal week. We found that in the presence of FPL, there was no significant change in eye-specific segregation in WT mice as compared to WT mice that had received either monocular or binocular injections of saline. However, these effects on segregation were highly variable leaving open the possibility that the efficacy of injections varied across mice.

4. Discussion

We demonstrated that the presence of an L-type calcium channel agonist induced robust correlated depolarizations in mice lacking the β2 subunit of the nAChR. However, application of FPL to β2−/− retina induced bursts of action potentials with highly variable burst properties and significantly lower nearest neighbor correlations as compared to WT mice. In addition, binocular injections of these agonists did not rescue eye-specific layer formation in β2−/− mice.

The goal of these experiments was to develop a reliable method of rescuing the various deficiencies in the visual system development of β2−/− mice. While FPL induced large correlated depolarizations in β2−/− RGCs (Figs. 1 and 2), these depolarizations had variable effects on the pattern of action potential within each cell (Fig. 3). In many cells, depolarizations were seen without any action potentials, while other neurons were induced to spike tonically. This variability in spiking pattern could be a reflection of FPL's effect on different cell types, each of which has a different complement of ion channels that contribute to these firing properties early in development (for reviews see, Robinson & Wang, 1998; Sernagor, Eglen, & Wong, 2001).

FPL induced synaptic currents in RGCs in β2−/− mice, suggesting a role for L-type channels in increasing synaptic release either directly by increasing $[Ca^{2+}]_i$ at synaptic release sites or indirectly by increasing presynaptic depolarization. In the adult retina, L-type channels are known to be involved in the release of neurotransmitter from cell classes that have sustained graded release, including photoreceptors and bipolar cells (Berntson, Taylor, & Morgans, 2003; Tachibana, Okada, Arimura, Kobayashi, & Piccolino, 1993). Since the effects of FPL can be seen in the absence of fast neurotransmission (Singer et al., 2001), the induced $[Ca^{2+}]_i$ transients that we see in β2−/− are unlikely to be from these cell types. Several classes of amacrine cell also express L-type channels (Habermann, O'Brien, Wassle, & Protti, 2003; Vigh, Solessio, Morgans, & Lasater, 2003, epublishing 2003, March 20; Xu, Zhao, & Yang, 2003) and may be involved in mediating the response to FPL. We are currently pursuing the hypothesis that the neuromodulator adenosine, which has been shown to modulate wave frequency (Stellwagen, Shatz, & Feller, 1999), is being released from amacrine cells to mediate $[Ca^{2+}]_i$ transients in the absence of fast neurotransmission.

The absence of spontaneous nAChR-mediated retinal activity prevents eye-specific segregation (Huberman et al., 2002; Huberman et al., 2003; Penn et al., 1998; Rossi et al., 2001)—however, identifying the essential features of retinal waves for driving this process is an area of ongoing research. Huberman et al. (2003) showed that intraocular injection of an immunotoxin for cholinergic amacrine cells disrupted RGC firing patterns but maintained periodic increases in calcium. Despite the disruption in the endogenous pattern of activity, immunotoxin-treated animals had normal formation of eye-specific layers. In contrast, between P1 and P8, β2−/− RGCs fire bursts of action potentials that are not correlated amongst neighboring cells (McLaughlin et al., 2003) and do not form eye-specific layers (Rossi et al., 2001; Muir-Robinson et al., 2002). Between P8 and P14, β2−/− retina have normal wave-like propagation of action potentials and local segregation of ipsilateral and contralateral axons into eye-specific regions, indicating that the absence of the β2 gene does not prevent plasticity in general. Based on these previous findings, we have hypothesized that some but not all features of the endogenous firing patterns is required for driving eye-specific refinement.

In vitro, FPL induced strong correlated depolarizations that led to significant increases in $[Ca^{2+}]_i$ (Figs. 1 and 2). FPL either prolonged RGC burst duration or moved the RGC into a depolarizing block and therefore inhibited robust RGC spiking (Fig. 3). Both the imaging and multielectrode array recordings revealed that bursts were roughly correlated. However, the variability on the effects of the firing properties of individual cells

prevented strong nearest neighbor correlations from being induced in β2−/− retina (Fig. 3). We found that repeated intraocular injections of FPL did not rescue eye-specific segregation in β2−/− mice. One explanation for this result is that the increased frequency of $[Ca^{2+}]_i$ transients and/or the change in action potential patterns relative to WT are not able to induce segregation.

Unfortunately, there are several confounding factors that limit our ability to interpret the effects of intraocular injections of FPL on eye-specific segregation. First, intraocular eye injections of FPL were toxic to β2−/−, which limited our ability to do repeated injections of high concentrations of FPL. Second, we must assume that the effects of FPL on the retina are similar in vivo and in vitro. We are unable to test this directly since there are no current mechanisms for recording spontaneous retinal activity in mice in vivo during the first postnatal week. Third, we do not know how long pharmacological effects last in vivo. We did observe a significant decrease in the extent of eye-specific segregation in β2−/− mice that received FPL injections (Fig. 4) indicating that the FPL was effective for some period of time.

In summary, we have characterized the activity patterns in the retina induced by the L-type calcium channel agonist FPL and concluded that they are inappropriate for rescuing eye-specific segregation in β2−/− mice. Perhaps more subtle manipulations, such as genetic mutations of L-type channels that mimic the effects of FPL, would be a more robust means of restoring activity patterns in β2−/− mice appropriate for driving map refinement.

Acknowledgments

We thank E.J. Chichilnisky for the mutlieletrode array and technical support. Supported in part by an NSF Graduate Research Fellowship, the Klingenstein Foundation, Whitehall Foundation, March of Dimes, McKnight Scholars Fund, and the National Institute of Health (grant no NS13528-01A1).

Supplementary material

Supplementary data associated with this article can be found, in the online version, at doi:10.1016/j.visres.2004.08.015.

References

Bansal, A., Singer, J. H., Hwang, B., & Feller, M. B. (2000). Mice lacking specific nAChR subunits exhibit dramatically altered spontaneous activity patterns and reveal a limited role for retinal waves in forming ON/OFF circuits in the inner retina. *Journal of Neuroscience, 20*, 7672–7681.

Berntson, A., Taylor, W. R., & Morgans, C. W. (2003). Molecular identity, synaptic localization, and physiology of calcium channels in retinal bipolar cells. *Journal of Neuroscience Research, 71*, 146–151.

Grubb, M. S., Rossi, F. M., Changeux, J. P., & Thompson, I. D. (2003). Abnormal functional organization in the dorsal lateral geniculate nucleus of mice lacking the beta 2 subunit of the nicotinic acetylcholine receptor. *Neuron, 40*, 1161–1172.

Habermann, C. J., O'Brien, B. J., Wassle, H., & Protti, D. A. (2003). AII amacrine cells express L-type calcium channels at their output synapses. *Journal of Neuroscience, 23*, 6904–6913.

Huberman, A. D., Stellwagen, D., & Chapman, B. (2002). Decoupling eye-specific segregation from lamination in the lateral geniculate nucleus. *Journal of Neuroscience, 22*, 9419–9429.

Huberman, A. D., Wang, G. Y., Liets, L. C., Collins, O. A., Chapman, B., & Chalupa, L. M. (2003). Eye-specific retinogeniculate segregation independent of normal neuronal activity. *Science, 300*, 994–998.

McLaughlin, T., Torborg, C. L., Feller, M. B., & O'Leary, D. D. (2003). Retinotopic map refinement requires spontaneous retinal waves during a brief critical period of development. *Neuron, 40*, 1147–1160.

Meister, M., Pine, J., & Baylor, D. A. (1994). Multi-neuronal signals from the retina: acquisition and analysis. *Journal of Neuroscience Methods, 51*, 95–106.

Muir-Robinson, G., Hwang, B. J., & Feller, M. B. (2002). Retinogeniculate axons undergo eye-specific segregation in the absence of eye-specific layers. *Journal of Neuroscience, 22*, 5259–5264.

Penn, A. A., Riquelme, P. A., Feller, M. B., & Shatz, C. J. (1998). Competition in retinogeniculate patterning driven by spontaneous activity. *Science, 279*, 2108–2112.

Picciotto, M. R., Zoli, M., Lena, C., Bessis, A., Lallemand, Y., LeNovere, N., et al. (1995). Abnormal avoidance learning in mice lacking functional high-affinity nicotine receptor in the brain. *Nature, 374*, 65–67.

Robinson, D. W., & Wang, G. Y. (1998). Development of intrinsic membrane properties in mammalian retinal ganglion cells. *Seminars in Cell and Development Biology, 9*, 301–310.

Rossi, F. M., Pizzorusso, T., Porciatti, V., Marubio, L. M., Maffei, L., & Changeux, J. P. (2001). Requirement of the nicotinic acetylcholine receptor beta2 subunit for the anatomical and functional development of the visual system. *Proceedings of National Academy Science USA, 98*, 6453–6458.

Sernagor, E., Eglen, S. J., & Wong, R. O. (2001). Development of retinal ganglion cell structure and function. *Progress in Retinal and Eye Research, 20*, 139–174.

Simon, D. K., Prusky, G. T., O'Leary, D. D., & Constantine-Paton, M. (1992). *N*-methyl-D-aspartate receptor antagonists disrupt the formation of a mammalian neural map. *Proceedings of the National Academy of Science USA, 89*, 10593–10597.

Singer, J. H., Mirotznik, R. R., & Feller, M. B. (2001). Potentiation of L-type calcium channels reveals nonsynaptic mechanisms that correlate spontaneous activity in the developing mammalian retina. *Journal of Neuroscience, 21*, 8514–8522.

Sretavan, D. W., Shatz, C. J., & Stryker, M. P. (1988). Modification of retinal ganglion cell axon morphology by prenatal infusion of tetrodotoxin. *Nature, 336*, 468–471.

Stellwagen, D., & Shatz, C. J. (2002). An instructive role for retinal waves in the development of retinogeniculate connectivity. *Neuron, 33*, 357–367.

Stellwagen, D., Shatz, C. J., & Feller, M. B. (1999). Dynamics of retinal waves are controlled by cyclic AMP. *Neuron, 24*, 673–685.

Tachibana, M., Okada, T., Arimura, T., Kobayashi, K., & Piccolino, M. (1993). Dihydropyridine-sensitive calcium current mediates neurotransmitter release from bipolar cells of the goldfish retina. *Journal of Neuroscience, 13*, 2898–2909.

Torborg, C. L., & Feller, M. B. (2004). Unbiased Analysis of Bulk Axonal Segregation Patterns. *Journal of Neuroscience Methods, 135*.

Torborg, C., Hansen, K., Feller, M. (2004). High frequency, synchronized bursting drives eye-specific segregation of retinogeniculate projections.

Vigh, J., Solessio, E., Morgans, C. W., & Lasater, E. M. (2003). Ionic mechanisms mediating oscillatory membrane potentials in wide-field retinal amacrine cells. *Journal of Neurophysiology, 90*, 431–443.

Wong, R. O., Meister, M., & Shatz, C. J. (1993). Transient period of correlated bursting activity during development of the mammalian retina. *Neuron, 11*, 923–938.

Xu, W., Orr-Urtreger, A., Nigro, F., Gelber, S., Sutcliffe, C. B., Armstrong, D., et al. (1999). Multiorgan autonomic dysfunction in mice lacking the beta2 and the beta4 subunits of neuronal nicotinic acetylcholine receptors. *Journal of Neuroscience, 19*, 9298–9305.

Xu, H. P., Zhao, J. W., & Yang, X. L. (2003). Cholinergic and dopaminergic amacrine cells differentially express calcium channel subunits in the rat retina. *Neuroscience, 118*, 763–768.